



Heavy Metals Distribution in the Serpentinite-Granite Contact Zone in El Sid Area, Central Eastern Desert, Egypt



Nour Eldin M. Gado*, Karim Abdelmalik and Abd El Moneim Osman

Geology Department, Faculty of Science, Ain Shams University, Cairo, Egypt

THE PRESENT work aims to investigate the heavy metal concentrations of the major rock units that exposed in El-Sid area, Central Eastern Desert, Egypt, and determine the hotspots areas with higher concentration levels in the investigated area. Concentrations of iron (Fe), zinc (Zn), lead (Pb), sulfur (S) and Arsenic (AS) were measured in the heavy mineral fractions of representative samples by using Atomic Absorption Spectrometer (AAS). The mapping of heavy metal concentrations was created by the inverse distance weighting (IDW) method. The highest concentrations of Fe, Zn and Pb were in Cataclastic granite, Monzo-Syenogranite and Qz-monzodiorite, while S is only detected in serpentinite after dunite rock. The present results showed that As was not detected in present samples. The lowest concentration of Fe was in carbonate rock stained with iron oxide and pyroxenite, Zn was in porphyritic meta-andesite, carbonate rock stained with iron oxide, serpentinite rocks and pyroxenite, and Pb was in serpentinite after dunite, serpentinite after pyroxenite with talc carbonate and pyroxenite. The results of the present study elucidate concentration levels of investigated heavy metals in rock units of the present area and refer to the hotspots areas with higher levels.

Keywords: Heavy Metals, EL-Sid, Atomic Absorption Spectrometer, Spatial Distribution.

1. Introduction

The Eastern Desert (ED) of Egypt is a notable region within the Arabian Nubian Shield (ANS), showcasing a prime illustration of many instances of granite magmatism (occurring between 750 to 550 million years ago) intruding subduction-related island arc and mafic-ultramafic rocks (known as supra subduction zone (SSZ) ophiolites). In the central and southern Eastern Deserts, granitoids and island-arc rocks are prevalent and constitute over 30% and 50% of the basement rocks, respectively. Gold deposits and occurrences are likely spread over the Central and Southern Eastern Desert as a result of granite magmatism's subsequent phases into potentially metal-bearing rocks. (Helmy et al., 2018).

Ophiolitic and granitic rocks are the dominant rock units in the research region. The ophiolitic rocks are composed of ultramafics (mostly serpentinites and Pyroxinites), mafic plutonic rocks (metagabbros), and metavolcanics (El-Sayed et al., 1999).

The present work aims to investigate the heavy metal concentrations of the major rock units that exposed in El-Sid area, Central Eastern Desert, Egypt, and determine the hotspots areas with higher concentration levels in the investigated area.

2. Materials and Methods

2.1. Study area

The study area is located in the central part of the Eastern Desert of Egypt about 90 Km to the west of El-Quseir city on the Red Sea coast. The area (**Fig. 1**) lies between latitude coordinates 25° 57' 00" 25° 59' 30" and longitudes 33° 36' 00" 33° 38' 00". The study area is accessible by the Qift - Quseir asphalt road, which traverses the Central Eastern Desert. The investigated area is distinguished by an arid climate that is dry and hot for most of the year, with minimal rainfall. The average temperature fluctuates from 12°C at night to more than 45°C during the day. The period of highest temperatures is long, ranging from May to September (Mohy, 2013).

2.2. Sampling, Sample preparation and analysis

The rock representative samples from the study area were sampled from 13 sites during the field survey (**Fig. 2**). The following procedures are applied to the rock sample to obtain the heavy minerals fractions required for atomic absorption analysis.

*Corresponding author e-mail: nourfouda@sci.asu.edu.eg

Received: 27/12/2024; Accepted: 09/01/2025

DOI: 10.21608/egjg.2025.348060.1101

©2025 National Information and Documentation Center (NIDOC)

2.2.1. Grinding of sample

For grinding rock samples, I used two different grinding techniques. The first technique is a mechanical jaw crusher, which initially grinds rock samples into sizable particles for further manual crushing via a hammer to end up with a grain size that is small enough to be inserted into ball mills. The second technique is Ball milling which is used for crushing material into finer particles and blending it thoroughly. There are two types of ball milling grinding wet and dry, Wet ball milling utilizes distilled water or anhydrous ethanol to move and carry the milling material in and out of the drum then put the sample in the dryer to eliminate distilled water from it. In contrast, dry ball milling does not use any liquid medium.

2.2.2. Sieving of grinding sample

After grinding, rock samples are sieved. Dry sieve analysis is the grain size test method used for the gravelly and sand-sized mineral samples. Sieve shakers assist particle movement through a stack of sieves, allowing for accurate particle separation. Depending on their size, the separated particles are retained on the various sieves. In the next step of the bromoform analysis, fine and very fine grain sizes that were retained from sieve sizes of 125 μm and 63 μm , respectively, are used.

2.2.3. Heavy mineral separation

Heavy minerals are mainly characterized by specific gravity greater than the medium which used to separate them from light minerals. The heavy liquid "bromoform" has a specific gravity of 2.89 at 20 °C (Hauff and Airey, 1980), which most commonly used medium for heavy mineral separation.

The following procedures are dependent on it for separating heavy minerals from rock samples by using bromoform liquid. as shown in (Fig. 3):

- Preparing the sample in the fine and very fine-grained size.
- Checking the specific gravity of bromoform before each use.
- Place the bromoform in a separate funnel with a glass tap that feeds into another funnel in which filter paper can be placed.
- Adding the subsample: stir occasionally to avoid mass-trapping effects (ensure grains are not removed on the stirring rod). Keep a watch glass over the funnel between stirrings. Allow 10-20 min for separation.
- Draining liquid with heavy minerals (with accompanying bromoform) into filter paper on the lower funnel; retain pure bromoform in storage bottle.

- Draining the rest of the bromoform together with light minerals into another filter paper; use the same storage bottle.
- Replacing the storage bottle with the bromoform washings bottle.
- Using alcohol. Wash residual bromoform and remaining grains from the upper funnel onto the lower filter paper. Then wash the bromoform from the filter paper.
- Washing the bromoform from the filter paper containing the heavy minerals into the same washing bottle. Both grains and filter paper should be clean of bromoform.
- Placing the filter paper and grains into bowls; air dry at a temperature no greater than 50 °C for 1-2 hours.
- Weighting both light and heavy mineral fractions.

2.2.4. Analysis of separated heavy mineral fractions

For each sample, one gram of heavy mineral fractions was digested in a mixture of nitric acid and hydrofluoric acid (2.5 ml of 70% HNO_3 and 2.5 ml of 35% HF) for 2 hours by using a Microwave Digestion System (CEM, MDS-2000, USA). After cooling to ambient temperature, the digested samples were filtered using the Whatman No.42 filter paper. The filtrated samples were diluted by deionized water to a concentration of 10%. Concentrations of iron (Fe), zinc (Zn), lead (Pb), sulfur (S) and Arsenic (AS) were measured in the samples by using Atomic Absorption Spectrometer (savant AA, GBC Scientific Equipment, Australia). Each sample was run in three replicates and the results were expressed in terms of $\mu\text{g/g}$ dry weight (mean \pm SD) (Oluyemi *et al.*, 2008). The analysis of heavy metals in rock samples was carried out in the central lab of the faculty of science, at Ain Shams University.

3. Results and Discussion

3.1. Concentrations of heavy metals in the samples

For atomic absorption analysis to determine the concentration of iron, zinc, lead, sulfur and arsenic as shown in Error! Reference source not found., one gram is the standard weight of heavy mineral fractions for each rock sample.

3.2. Column Charts

Data representation is essential for displaying the results of the processed data. Data are visualized using column charts.

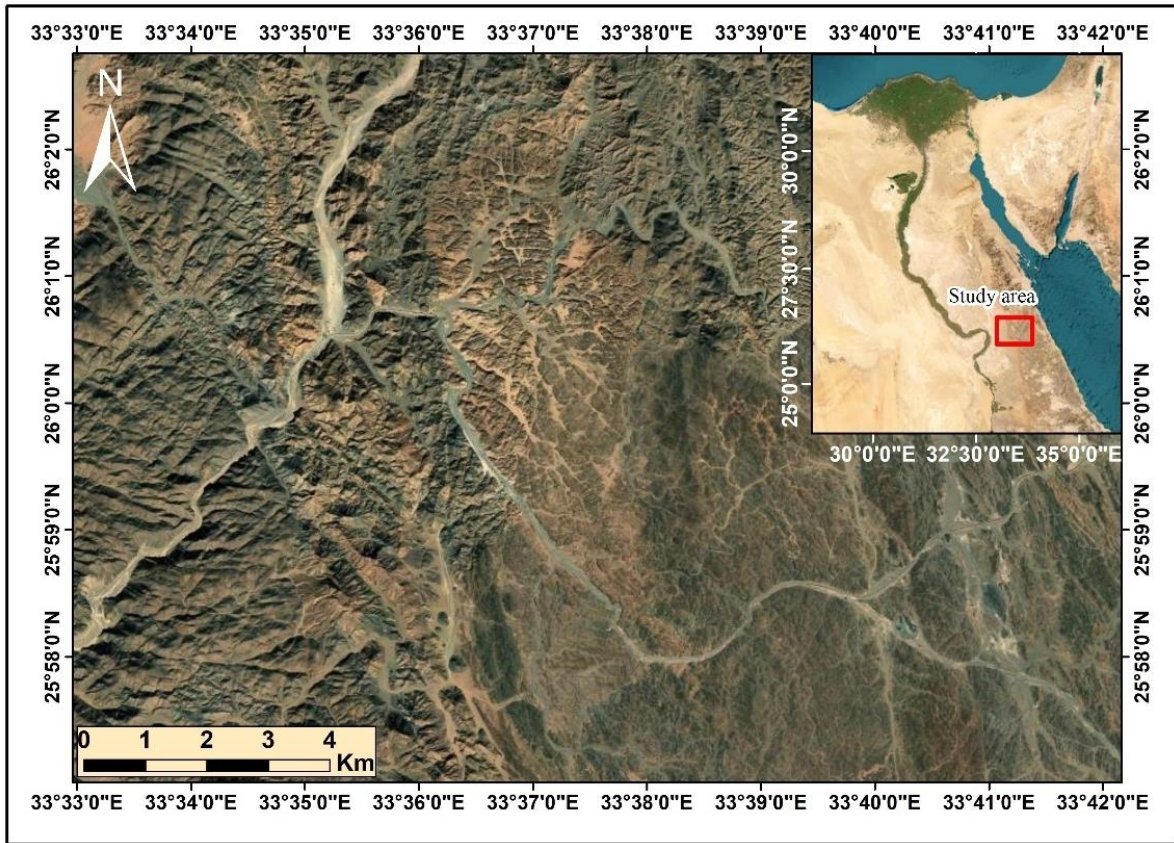


Fig. 1. Location map of the study area.

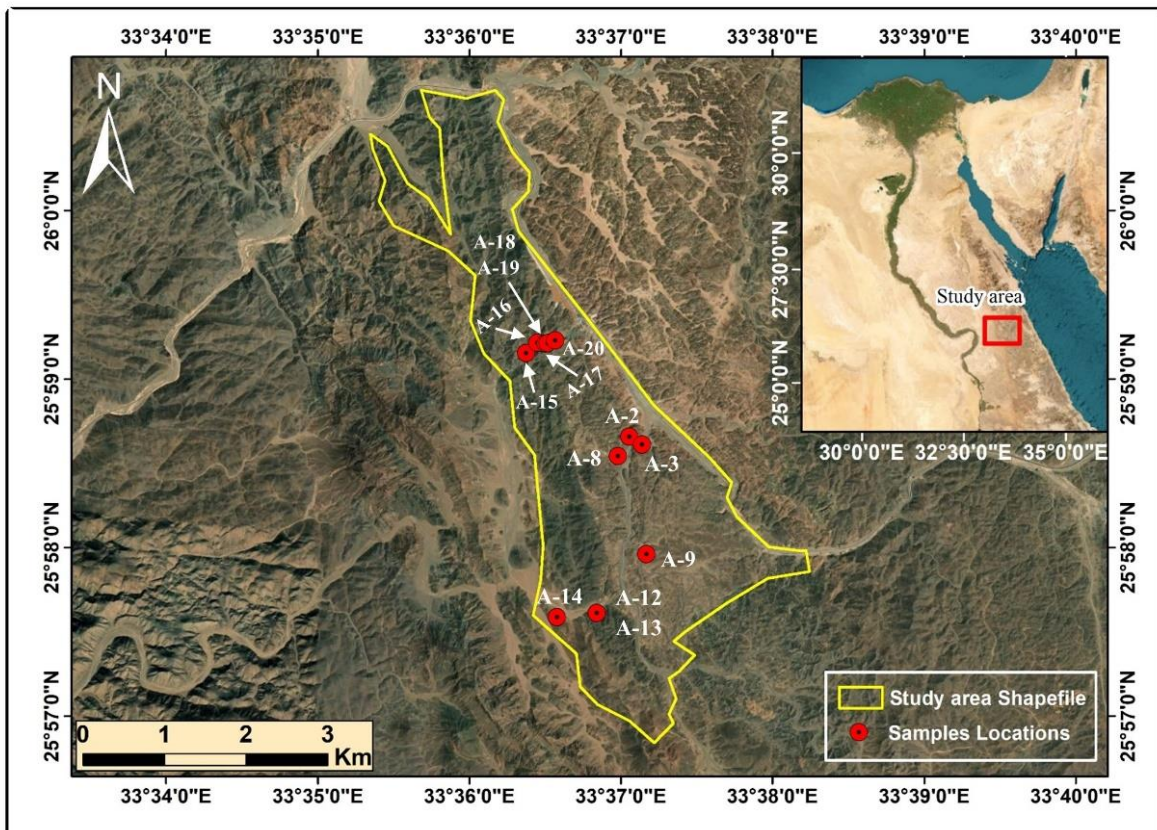


Fig. 2. The spatial distribution Map of the stations where representative samples were collected.

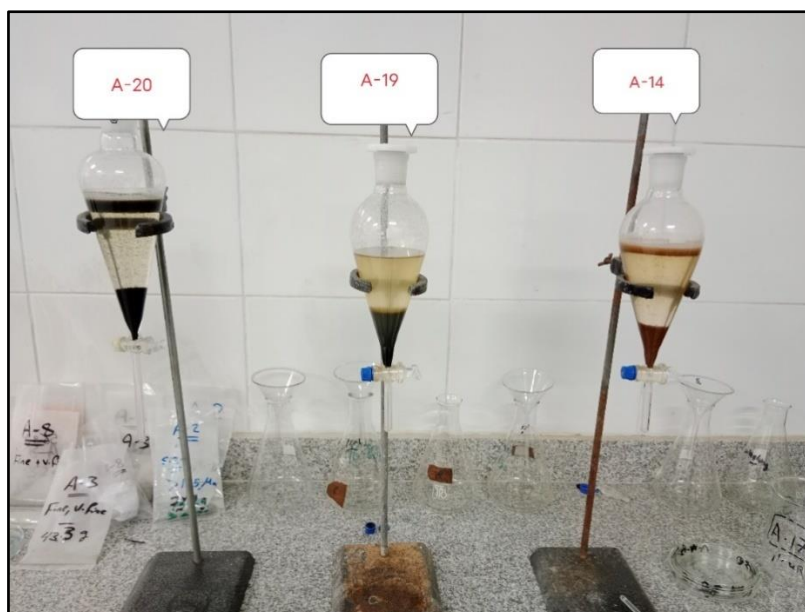


Fig. 3. Heavy minerals separation of samples by bromoform.

Table 1. Fe, Zn, Pb, S and As concentrations for heavy mineral fractions for each rock sample with a standard weight of one gram. ND: Not Detect.

Sample ID	Rock name	Fe %	Zn (mg/Kg)	Pb (mg/Kg)	S%	As (mg/Kg)
A-2	Cataclastic granite	19.99	218.47	55.11	N.D	
A-3	Monzo-Syenogranite	26.67	619.13	62.47	N.D	
A-8	Qz- monzodiorite	21.56	332.01	52.53	N.D	
A-9	Porphyritic meta-andesite	10.93	66.08	54.11	N.D	
A-12	Metagabbro	10.32	109.43	43.77	N.D	
A-13	Metabasalt	15.22	161.62	39.87	N.D	
A-14	Carbonate rock stained with iron oxide	2.02	34.86	41.74	N.D	
A-15	High altered metagabbro	12.78	101.31	45.35	N.D	N.D
A-16	serpentinite after dunite	17.29	47.78	36.33	1.08	
A-17	serpentinite after pyroxenite	22.73	59.31	41.51	N.D	
A-18	Serpentinite after pyroxenite with talc carbonate.	8.62	62.05	38.71	N.D	
A-19	pyroxenite	1.98	54.57	34.29	N.D	
A-20	High-altered granite at the gold mine	17.56	318.82	44.83	N.D	

The representation charts for the Fe, Zn, and Pb concentrations of heavy mineral fractions for each rock sample with standard weight one gram as shown in **Fig. 4**, **Fig. 5** and **Fig. 6** respectively. The elements concentration chart of Fe, Zn, and Pb of heavy mineral fractions for all samples with a standard weight of one gram for each sample as shown in **Fig. 7**.

3.3. Scatter plot diagrams

Scatter plot diagrams show the relationship between

In **Fig. 8** the values of lead increase as the values of iron. The correlation coefficient (r) between Pb and Fe is 0.59, indicating a moderately positive correlation according to **Table 2**. In **Fig. 9** The values of zinc increase as the values of iron. The correlation coefficient (r) between Zn and Fe is 0.69, indicating a moderately positive correlation according to **Table 2**. In **Fig. 10** The values of lead increase as the values of zinc. The correlation coefficient (r) between Pb and Zn is 0.74, indicating a higher positive correlation according to **Table 2**.

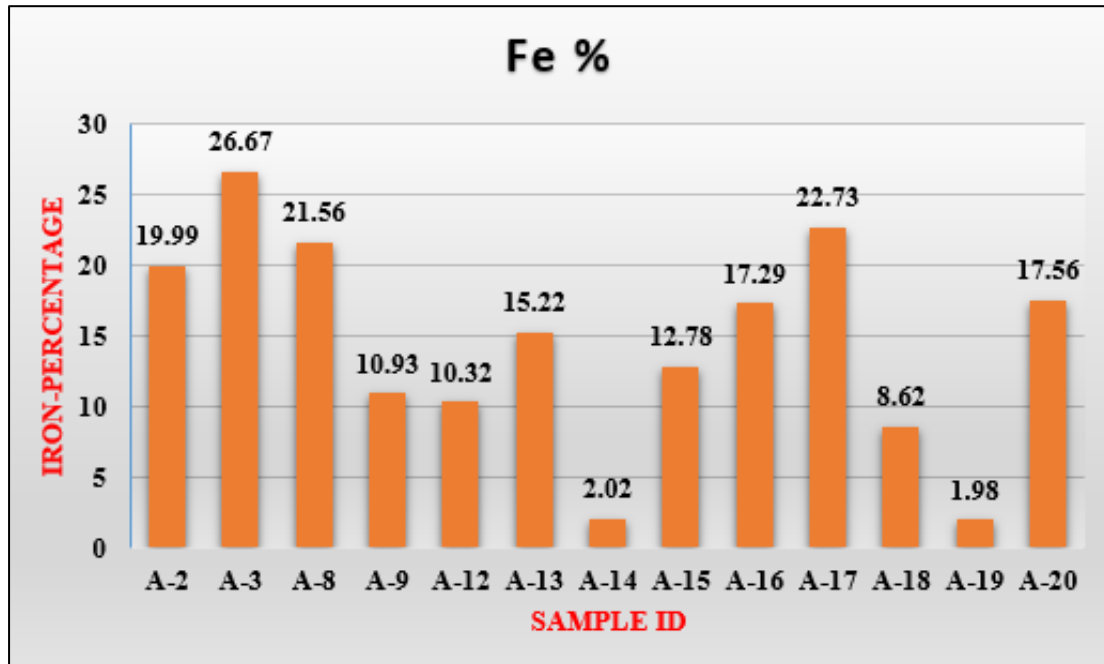


Fig. 4. Chart of iron concentration (%) of heavy mineral fractions for each rock samples with a standard weight of one gram.

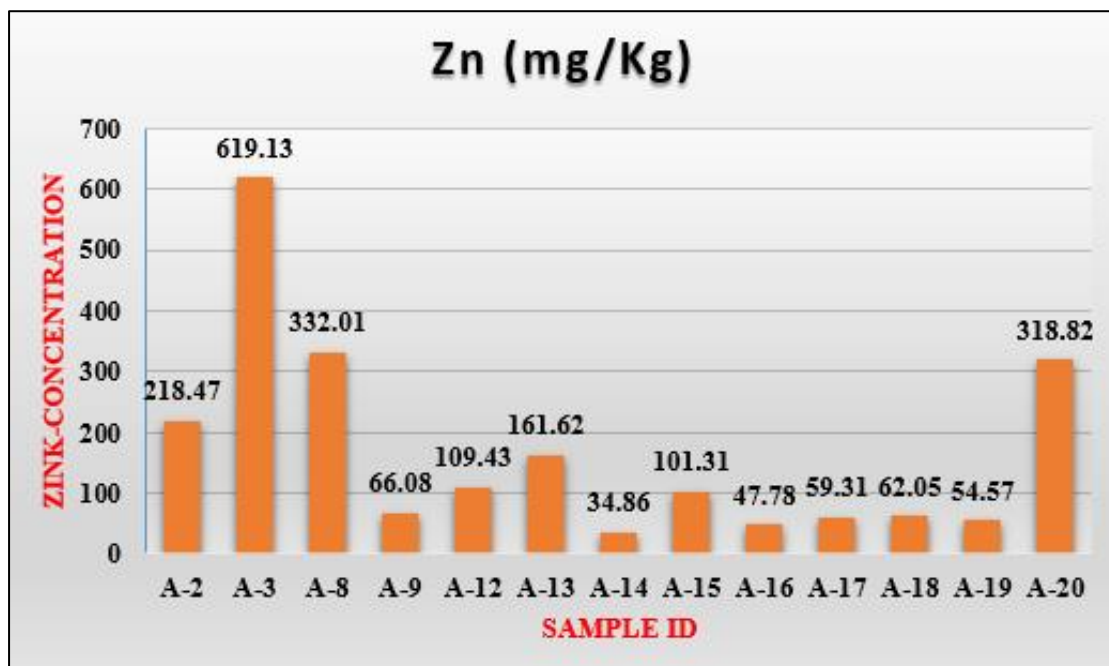


Fig. 5. Chart of zinc concentration (mg/Kg) of heavy mineral fractions for each rock samples with a standard weight of one gram.

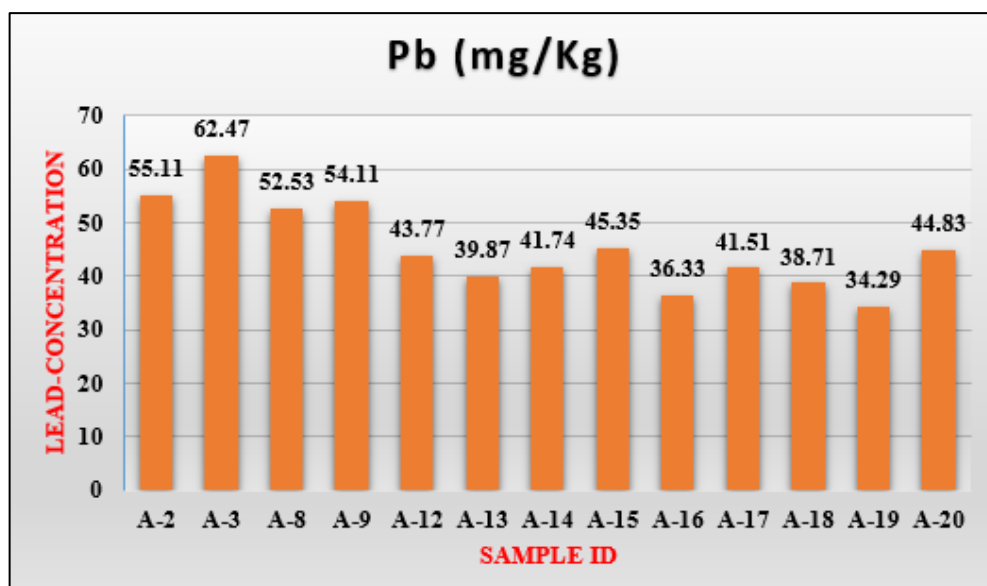


Fig. 6. Chart of lead concentration (mg/Kg) of heavy mineral fractions for each rock samples with a standard weight of one gram.

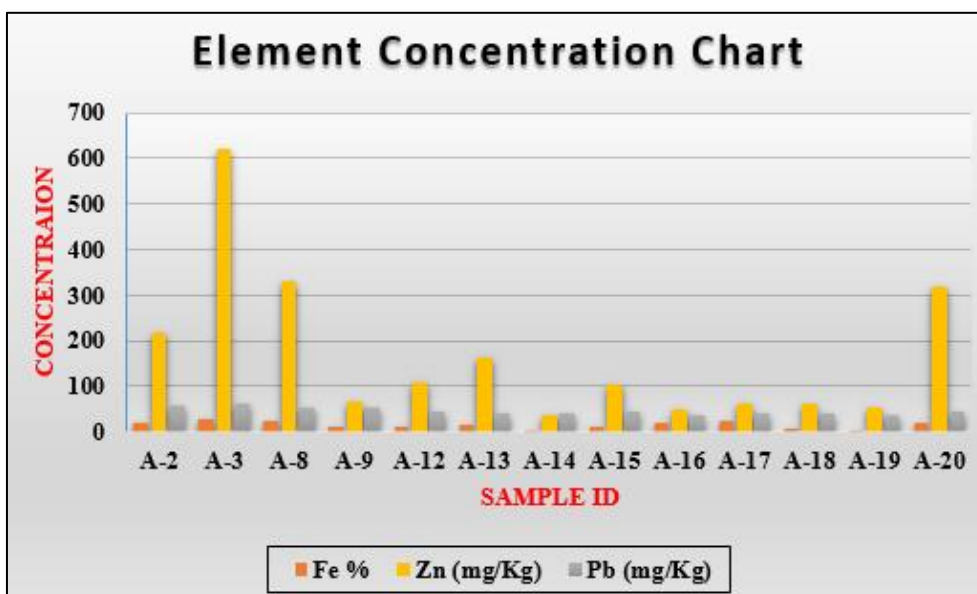


Fig. 7. Elements concentration chart for Fe, Zn and Pb of heavy mineral fractions for each rock samples with a standard weight of one gram.

Table 2. Rule of Thumb for interpreting the size of a correlation coefficient (after Mukaka, 2012).

Size of correlation	Interpretation
0.90 to 1.00 (-0.90 to -1.00)	Very high positive (negative) correlation
0.70 to 0.90 (-0.70 to -0.90)	High positive (negative) correlation
0.50 to 0.70 (-0.50 to -0.70)	Moderate positive (negative) correlation
0.30 to 0.50 (-0.30 to -0.50)	Low positive (negative) correlation
0.00 to 0.30 (0.00 to -0.30)	negligible correlation

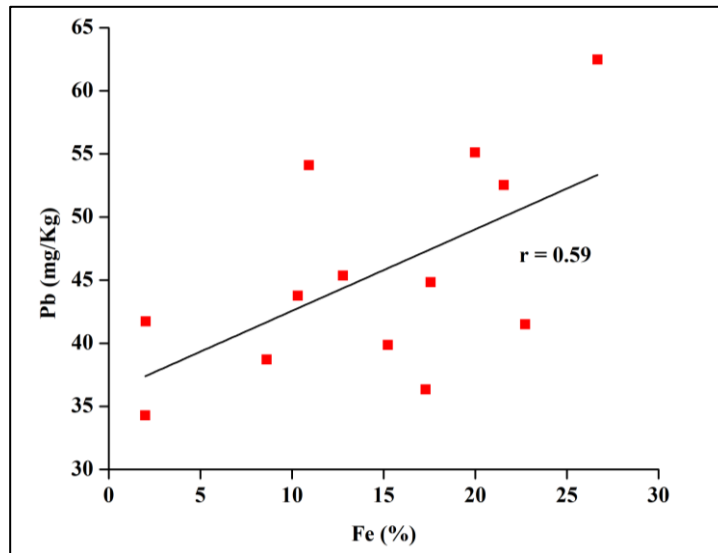


Fig. 8. Scatter plot of iron (Fe) and Lead (BP).

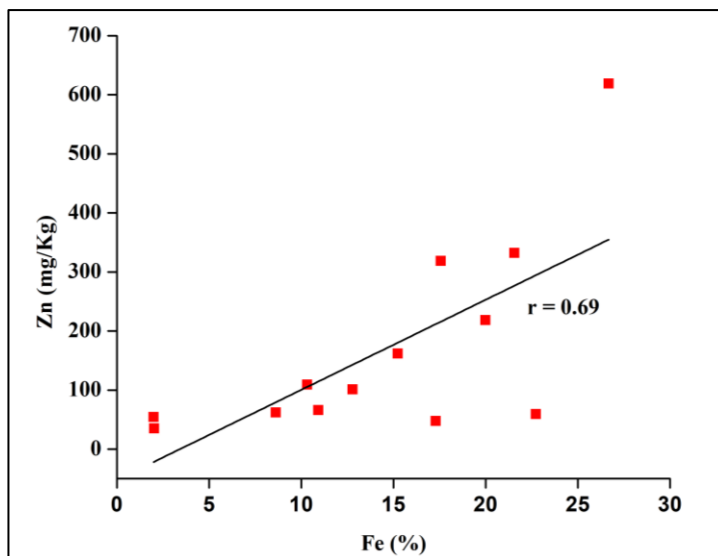


Fig. 9. Scatter plot of iron (Fe) and Zinc (Zn).

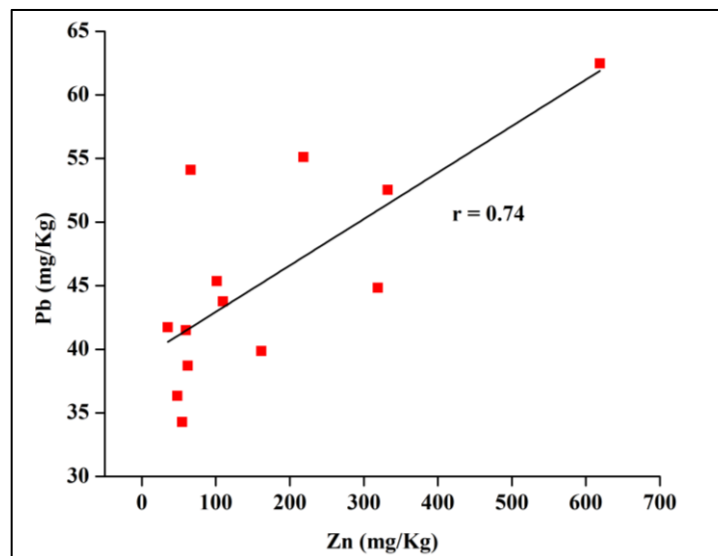


Fig. 10. Scatter plot of Zinc (Zn) and Lead (Pb).

3.4. Spatial distribution maps

Spatial distribution maps utilize cartographic representation approaches to clarify the spatial relationships between distributed phenomena on maps. It accurately depicts economic, environmental, and geological issues, facilitating scientific representation and analysis (Abou El-Anwar et al. 2024). These maps are considered more accurate and more valuable than traditional descriptive approaches because they display the quantitative results on the maps to demonstrate the spatial variation in the distribution of the examined phenomena (e.g., element concentration distribution) (Salman et al. 2019a, b &c; Salman and Elnazer 2020; Selem et al. 2021; Salman et al. 2021; Abou El-Anwar et al. 2024). There are two groups of interpolation methods.

Deterministic and Geostatistical interpolation methods, the IDW is the optimal and most significant interpolation method (Al-Mamoori et al., 2021). The inverse distance weighting (IDW) method is used in mapping of Fe, Zn and Pb concentrations in the study area. The IDW is one of the most widely used and deterministic interpolation techniques. IDW calculations were based on nearby, well-known locations. The weights given to the interpolating points are inversely proportional to their separation from the interpolating point. As a result, the close points are created have higher weights (and thus, greater impact) than the distant points, and vice versa (Bhunja et al., 2018). Fig. 11. display the spatial distribution maps of the concentrations of Fe, Pb, and Zn in the study area, respectively.

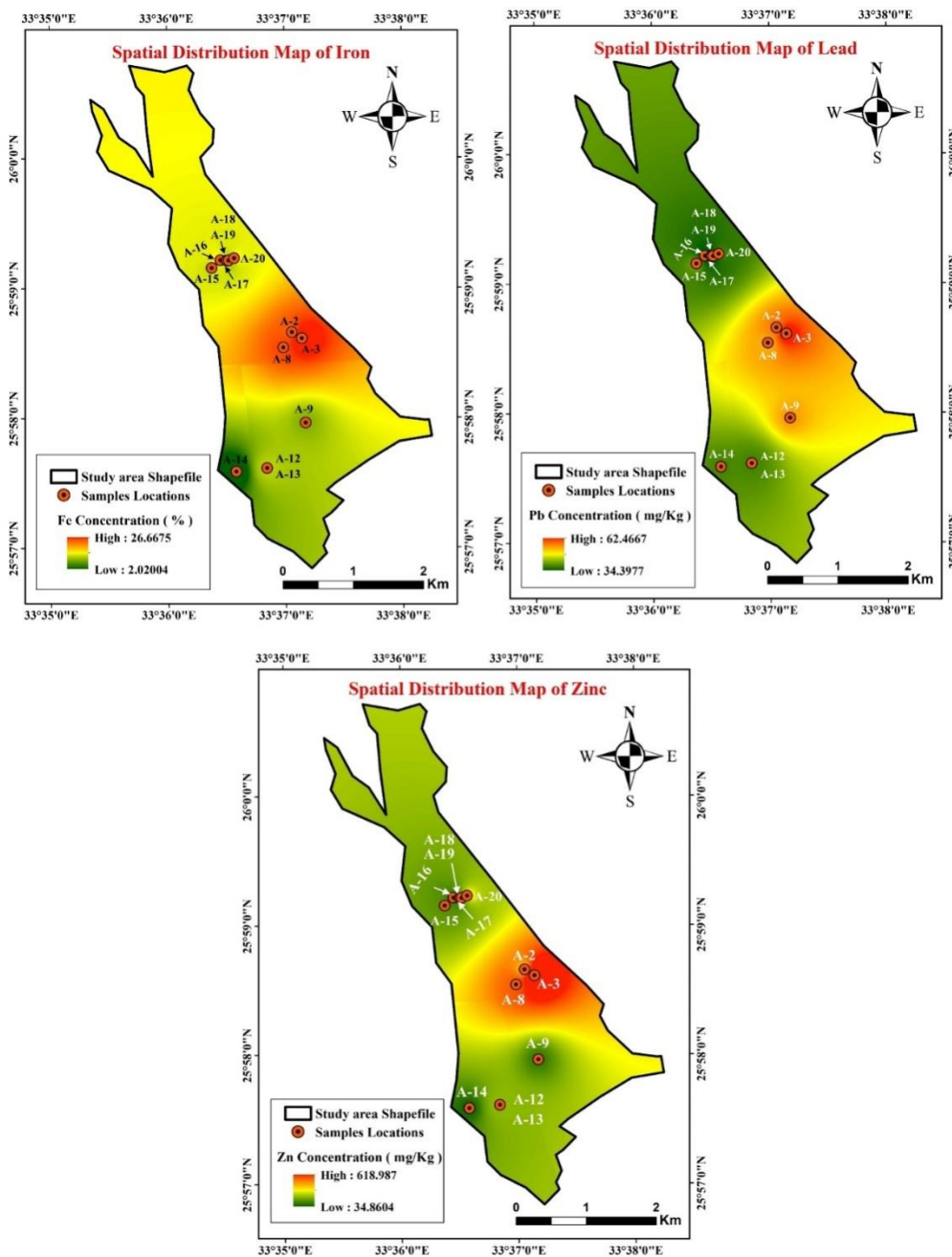


Fig. 11. Spatial distribution maps of iron, lead and Zinc concentrations.

The highest concentrations of Fe, Zn and Pb were found in Cataclastic granite, Monzo-Syenogranite and Qz-monzodiorite, while S is only detected in serpentinite after dunite rock. The present results showed that As was not detected in our samples.

The lowest concentration of Fe was found in carbonate rock stained with iron oxide and pyroxenite, whereas Zn was present in porphyritic meta-andesite, carbonate rock stained with iron oxide, serpentinite rocks and pyroxenite. Pb was detected in serpentinite after dunite, serpentinite after pyroxenite with talc carbonate and pyroxenite.

4. Conclusions

Results of this study have provided the heavy metal concentrations of the major rock units that exposed in El-Sid area, Central Eastern Desert, Egypt, and have determined the hotspots areas with higher concentration levels in the investigated area.

Ethics approval and consent to participate: This article does not contain any studies with human participants or animals performed by any of the authors.

Consent for publication: All authors declare their consent for publication.

Conflicts of Interest: The author declares no conflict of interest.

Contribution of Authors: All authors shared in writing, editing and revising the MS and agree to its publication.

5. References

- Abou El-Anwar, E.A., Belal, Z.L., Seleem, E. M., and Salman, S. A. (2024). Central Nile Valley agriculture soil content and distribution of rare earth elements (REEs), Egypt. *Egyptian Journal of Geology*, 68(1), 35-46.
- Al-Mamoori, S. K., Al-Maliki, L. A., Al-Sultani, A. H., El-Tawil, K and Al-Ansari, N. (2021). Statistical analysis of the best GIS interpolation method for bearing capacity estimation in An-Najaf City, Iraq. *Environmental Earth Sciences*, 80 (20), 1-14. <https://doi.org/10.1007/s12665-021-09971-2>
- Bhunia, G. S., Shit, P. K., and Maiti, R. (2018). Comparison of GIS-based interpolation methods for spatial distribution of soil organic carbon (SOC). *Journal of the Saudi Society of Agricultural Sciences*, 17 (2), 114-126. <https://doi.org/10.1016/j.jssas.2016.02.001>.
- El-Sayed, M. M., Furnes, H., and Mohamed, F. H. (1999). Geochemical constraints on the tectonomagmatic evolution of the late Precambrian Fawakhir ophiolite, Central Eastern Desert, Egypt. *Journal of African Earth Sciences*, 29 (3), 515-533. [https://doi.org/10.1016/S0899-5362\(99\)00113-X](https://doi.org/10.1016/S0899-5362(99)00113-X).
- Hauff, P. L. and Airey, J. (1980). The handling, hazards, and maintenance of heavy liquids in the geologic laboratory. US Geological Survey, Circular, 827.
- Helmy, H. M., Elshafei, S., and Elwan, W. (2018). Journal of African Earth Sciences Mineralogy and geochemistry of metasomatized mantle peridotites from the Eastern Desert of Egypt: The role of granite-related hydrothermal fluids in gold mineralizations. *Journal of African Earth Sciences*, 144, 136-150. <https://doi.org/10.1016/j.jafrearsci.2018.04.003>.
- Mohy, H., (2013): Application of remote sensing for gold exploration in the Fawakhir area, Central Eastern Desert of Egypt. Msc Thesis, Faculty of Science, Cairo University., Egypt, 151.
- Mukaka, M.M. (2012). Statistics Corner: A Guide to Appropriate Use of Correlation Coefficient. *Malawi Medical Journal*, 24 (3), 69-71. <https://pubmed.ncbi.nlm.nih.gov/23638278/>.
- Oluyemi, E. A., Feuyit, G. J. A. I., Oyekunle, J. A. O., and Ogunfowokan, A. O. (2008). Seasonal variations in heavy metal concentrations in soil and some selected crops at a landfill in Nigeria. *African Journal of Environmental Science and Technology*, 2 (5), 089-096.
- Salman, S. A., Zeid, S. A., Seleem, E. M. M., and Abdel-Hafiz, M. A. (2019). Soil characterization and heavy metal pollution assessment in Orabi farms, El Obour, Egypt. *Bulletin of the National Research Centre*, 43, 1-13.
- Salman S.A., Arauzo M., Elnazer, A.A. (2019a). Groundwater quality and vulnerability assessment in west Luxor Governorate, Egypt, *Groundwater for Sustainable Development*, 8, 271-280.
- Salman, S.A., Zeid, S.A.M., Seleem, E.M., and Abdel-Hafiz, M.A. (2019b). Soil Characterization and Heavy Metal Pollution Assessment in Orabi Farms, El Obour, Egypt. *Bulletin of the National Research Centre* 43, 1-13, <https://doi.org/10.1186/s42269-019-0082-1>
- Salman, S.A., Asmoay, A.S., El-Gohary, A.M., and Sabet, H.S. (2019c). Evaluation of human risks of surface and groundwater contaminated with Cd and Pb south of El-Minya Governorate, Egypt. *Drinking Water Engineering and Science* 12, 23-30., <https://doi.org/10.5194/dwes-12-23-2019>.
- Salman S.A. and Elnazer, A.A. (2020). Assessment and speciation of chromium in groundwater of south Sohag Governorate, Egypt. *Groundwater for Sustainable Development*, 10, 100369, doi.org/10.1016/j.gsd.2020.100369.
- Salman, S.A., Abou El-Anwar, E.A., Asmoay, A.S., Mekky, H.S., Abdel Wahab W., and Elnazer, A.A. (2021). Chemical Fractionation and Risk Assessment of Some Heavy Metals in Soils, Assiut Governorate, Egypt. *Egyptian Journal of Chemistry*, 64(7), 3311-3321. DOI: 10.21608/EJCHEM.2021.59371.3276
- Seleem E.M., Alaa Mostafa A., Mokhtar M., Salman S.A. (2021). Risk assessment of heavy metals in drinking water on the human health, Assiut city and its environs, Egypt. *Arabian Journal of Geosciences* 14, 1-11, doi: 10.1007/s12517-021-06784-2

توزيع الفلزات الثقيلة في نطاق تماس السربنتين والجرانيت في منطقة السد، وسط الصحراء الشرقية، مصر

نور الدين محمد جادو، وكريم عبدالمالك، وعبدالمنعم عثمان

قسم الجيولوجيا، كلية العلوم، جامعة عين شمس، القاهرة، جمهورية مصر العربية

يهدف العمل الحالي إلى التحقيق في تراكيز المعادن الثقيلة للوحدات الصخرية الرئيسية المعرضة في منطقة السد، وسط الصحراء الشرقية، مصر، وتحديد مناطق النقاط الساخنة ذات مستويات التركيز الأعلى في المنطقة التي تم فحصها. تم قياس تراكيز الحديد (Fe) والزنك (Zn) والرصاص (Pb) والكبريت (S) والزرنيخ (AS) في الأجزاء المعدنية الثقيلة للعينات الممتلئة باستخدام مطياف الامتصاص الذري (AAS). تم إنشاء رسم خرائط تراكيز المعادن الثقيلة بواسطة طريقة الترجيح العكسي للمسافة (IDW). كانت أعلى تراكيز Fe و Zn و Pb في كتاكلاستيك و كوارتز مونزوديوريت ومونزو سينوجرانيت ، بينما تم اكتشاف S فقط في السربنتين الناتجة من تحول اللاوليفين. أظهرت النتائج الحالية أنه الزرنيخ AS لم يتم اكتشافها في العينات الحالية. كان أقل تركيز لـ Fe في صخور الكربونات المصبغة بأكسيد الحديد والبيروكسينيت، وكان Zn في ميتا أنديسيت البورفيريتي، وصخور الكربونات المصبغة بأكسيد الحديد، وصخور السربنتين والبيروكسينيت، وكان Pb في السربنتين الناتجة من تحول اللاوليفين ، و السربنتين الناتجة من تحول البيروكسين المصاحب بتلك وكربونات ، البيروكسينيت. توضح نتائج هذه الدراسة مستويات تركيز المعادن الثقيلة التي تم فحصها في الوحدات الصخرية في المنطقة الحالية وتشير إلى مناطق النقاط الساخنة ذات المستويات الأعلى.